Journal of Physics: Conference Series

PAPER • **OPEN ACCESS**

Robust DWT-SVD Domain Image Watermarking based on Iterative Blending

To cite this article: Kodathala Sai Varun *et al* 2021 *J. Phys.: Conf. Ser.* **2070** 012111

Robust DWT-SVD Domain Image Watermarking based on Iterative Blending

Kodathala Sai Varun[1], Ajay Kumar Mandava[1], Rakesh Chowdary[1]

[1] Department of Electrical, Electronics and Communication Engineering, GITAM School of Technology, GITAM, Bengaluru Campus, Karnataka, India

E-mail: kodathalasaivarun@gmail.com

Abstract. Copyright protection for digital multimedia has become a research hotspot in recent years. As an efficient solution, the digital watermarking scheme has emerged at the right moment. In this article, a highly robust and hybrid watermarking method is proposed. The discrete wavelet transform (DWT) and the singular value decomposition (SVD) as well as iterative blending are adopted in this method to insert and recover the watermark. To enhance the watermark imperceptibility, the second low-level (LL2) coefficients after SVD are modified by using the watermark. Compared with the conventional DWT-SVD-based watermarking method and other watermarking techniques, the watermarked images obtained by the proposed method have higher image quality. In addition, the proposed method achieves high robustness in resisting various image processing attacks.

1. Introduction

Digital Image watermarking has gained interest due to both its abundance and the method of distribution. These methods guard against unauthorized access and misuse of digital information. Authentication, operator acknowledgment, material preservation, and trademark protection are all applications that involve these techniques. Watermarking approaches for digital images vary according to the working domain (spatial, frequency, or hybrid), the type of document (text, picture, audio, or video), the algorithm utilized (sequential or parallel), human perceptibility (visible or invisible), and the type of application (i.e., source or destination-based). This section summarizes current developments in this area and covers various strategies for digital picture watermarking based on the working domain. The techniques for watermarking of the spatial domain are too fragile to control. These methods are significantly less resistant to various forms of attacks than frequency-domain algorithms. These disadvantages have prompted researchers to investigate transform-domain watermarking techniques that more effectively conceal data in the transform space of a signal rather than in its time domain. This technique converts an image to the frequency domain using a predefined transform. The watermark is then embedded by altering the original image's transform domain coefficients using various transformations, including the Discrete Cosine Transform (DCT), the Discrete Fourier Transform (DFT), the Discrete Wavelet Transform (DWT), and the Singular Value Decomposition (SVD). Finally, it extracts the watermark using an inverse transformation and a right key. Singular value decomposition (SVD) has gained much attention in watermarking theory due to its stability in signal processing. The SVD traditional robust watermark approach was introduced in [1] by Liu and Tan. By modulating the singular values of the image directly, the watermark is inserted into the carrier image. However, this approach is not safe enough and the watermark has a lot to do with image quality. To solve the problem there have been several robust watermarking processes that combine SVD with other transforms including DWT and DCT based on hybrid transformation has been proposed. Lai and Tsai [2] proposed a DWT- SVD-based watermarking algorithm that inserts the watermark by changing the singular values of high-frequency sub-bands. Gupta and Raval suggested another DWT-SVD-based robust watermarking approach in [3]. The principal component of the watermark is then superimposed on the singular values of the diagonal high-frequency sub-band in this scheme (HH). However, experimental findings show that when the watermark images have been attacked, the extracted watermark has low image quality. Narula et al. compared the performance of the DWT and DWT-SVD watermarking schemes in RGB images in [4], concluding that the hybrid DWT-SVD based scheme outperforms the traditional DWT based scheme.

In [5], the authors suggested a DWT-based image watermarking scheme. In this paper, the watermark is incorporated into the first-level decomposition coefficients, however, the image quality degrades with increased quantization steps Jinyuan et al. [6] proposed a logistic map- based watermarking algorithm for digital images in the DWT domain. The watermark bit is then incorporated into the multilevel DWT coefficients. However, the PSNR of this approach is low, and the trade-off between robustness and imperceptibility is unsatisfactory. Asma et al. [7] proposed a DWT-based approach that uses alpha blending to insert a watermark bit into the low-frequency band. This form, however, is the least robust against Gaussian noise. Hsieh and Tseng [8] suggested the following steps for a DWT-based algorithm: The wavelet coefficients of an original image are decomposed. Then, to achieve a robust algorithm, a multi- energy watermarking scheme based on the suitable significant wavelet tree is used. Rastiet al. embedded the watermark using DWT, SVD, orthogonal-triangular decomposition, and chirpz- transform [9]. DWT is applied at two levels, and the LL sub-band is chosen to embed the watermark's unique values. Roy et al. proposed a new watermarking approach based on the YCbCr colour space using DWT and SVD [10]. The Cb component is chosen and subdivided into four-level sub bands. The HL sub-band is chosen to embed the watermark's unique values. Lakritz et al. [11] proposed a dynamic watermarking which used three levels of DWT for the luminance value of the host image, and then he divided the sub band LL into many blocks. A dynamic block is randomly picked for embedding using a pseudo-random generator. Ali et al. [12] proposed a DWT/SVD hybrid picture watermarking system. The host image is subjected to a two-level DWT, followed by SVD on all sub-bands. On each sub-band, the watermark is modified using 1-level DWT followed by SVD. The principal components for each sub-band in the watermark are then determined. Finally, in the converted host image, the primary components of each sub-band are incorporated in the singular values S of each sub- band. To achieve imperceptibility and robustness, DE is employed to obtain the best MSF. The principal components are employed instead of singular values, hence FPP is avoided. The hybrid SVD-Based image watermarking systems have been examined by W H. Alshoura et al. [13]. The survey focussed on SVD and hybrid frequency domains systems and assessed existing watermarking systems. The study involved SVD security vulnerabilities (FTP attacks), hybrid SVD classification, and SVD embedding comparison.

This paper is structured as follows. In Section 2, we go over the fundamentals of discrete wavelet transforms (DWT). In Section 3, we present our new DWT-based watermarking system. In Section 4, we carry out some numerical experiments with various image distortions and finally the conclusion.

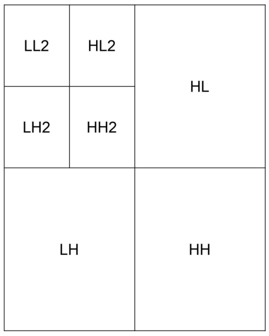

Figure 1. 2 – Level DWT decomposition

2. The wavelet transform, SVD and iterative blending

In this section the mathematical description of Discrete Wavelet Transform (DWT), Singular Value Decomposition (SVD) and the Iterative blending is summed up concisely. The broad description about the techniques can be fetched from [14], [15] and [16].

2.1. The Wavelet Transform

Discrete wavelet transform is a technique which transforms image pixels into wavelets. These wavelets are then used for wavelet-based compression and coding. The DWT is defined as [17]:

$$W_{\varphi}(j_0, k) = \frac{1}{\sqrt{M}} \sum_{x} f(x) \varphi_{j_0,k}(x) \tag{1}$$

In two - dimensional DWT, the matrix is decomposed into four sub-bands namely: LL,HL, LH, HH. The sub-band LL can be further decomposed to obtain second level of decomposition. The process is continued until the desired level of decomposition is reached. To preserve the properties of imperceptibility and robustness 2^{nd} level decomposition is applied on both the host and watermark images and the second level - low level features (LL2 sub-bands) are used for embedding.

2.2. Singular Value Decomposition

Singular value decomposition (SVD) is a technique which is extensively used to decompose a matrix into several component matrices. SVD of a real matrix A is defined as

$$[A] = [U][S][V]^T \tag{2}$$

Matrices [U] and [V] consists of left and right singular vectors of [A] and the diagonal elements of [S] are the singular values of [A]. The SVD is applied on the LL2 sub-bands and the corresponding singular matrices are used for embedding, the advantage of using SVD is the decomposed singular matrix is robust against geometric attacks.

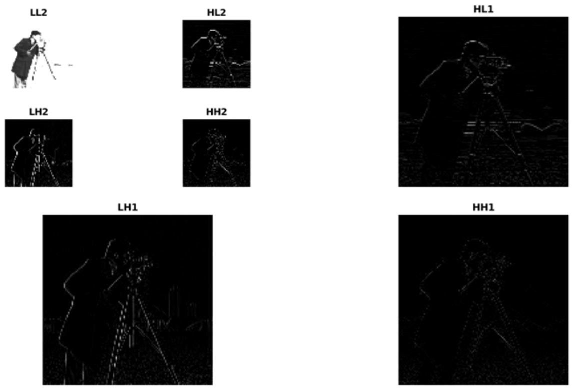

Figure 2. DWT decomposition of cameraman

2.3. The Iterative Blending

Zhang Gui-cang, Wang Rang-ding and Zhang Yujin [16] proposed a digital image information hiding technique using iterative blending in intensity domain. If H and W are host and watermark images respectively then the iterative embedded image E is given by

$$E(x, y) = (1 - \alpha^n) * H(x, y) + \alpha^n * W(x, y) \tag{3}$$

Where α is the embedding strength parameter ($0 < \alpha < 1$) and n is the number of iterations. The embedding strength α decides the strength of watermark being embedded and n describes the host image concentration. The following are the properties of iterative blending:

1. The difference between embedded image E and host image H is inversely proportional to number of iterations and directly proportional to α :

$$\Delta(E - H) \propto \frac{\alpha}{n} \tag{4}$$

2. The difference between extracted watermark W' and original watermark W is directly proportional to number of iterations and inversely proportional to α:

$$\Delta(W' - W) \propto \frac{n}{\alpha} \tag{5}$$

3. From the property 1, the embedded image is equal to the host image as $n \to \infty$.

From the properties, parameters α & n must be chosen wisely in order to maintain robustness and imperceptibility. This iterative blending algorithm is applied on the singular matrix in the transform domain to approach high robustness and imperceptibility. A new hybrid non-blind image watermarking system is proposed in this paper, which integrates DWT, SVD, and iterative blending and is robust to various attacks.

3. The proposed watermarking technique

In this section, the embedding and extracting process used to achieve high quality metrics are defined.

3.1. Embedding process

The embedding process requires pre-processing of both host and watermark images, the both images are converted to monochrome and default input size is set to [256,256] which can be varied. It is required to resize both the images to same dimensions. The detailed embedding process is given in *Algorithm: 1*.

Algorithm 1: Watermark embedding process

Input:
- **(i) Load Host Image H.**
- **(ii) Load Watermark Image W.**
- **(iii) Choose embedding parameters α, n.**

Embedding Process:
- **(i) Apply DWT on Host image H to get LL, HL, LH, HH.**
- **(ii) Apply second level DWT on LL sub-band to get LL2, HL2, LH2, HH2.**
- **(iii) Apply SVD on LL2:** $LL2 = U * S * V'$.
- **(iv) Apply DWT on Watermark image W to get LLw, HLw, LHw, HHw.**
- **(v) Apply second level DWT on LLw sub-band to get LLw2, HLw2, LHw2, HHw2.**
- **(vi) Apply SVD on LLw2:** $LLw2 = Uw * Sw * Vw'$.
- **(vii) Modify S matrix using:** $S' = (1 - \alpha^n) * S + \alpha^n * (S_w)$.
- **(viii) Reconstruct LL2':** $LL2' = U * S' * V'$.
- **(ix) Apply two times inverse DWT to construct Embedded Image E.**

Output: Embedded Image E

3.2. Extraction process

The extraction process is inverse embedding process and detailed description is given in *Algorithm : 2*.

Algorithm 2: Watermark extraction process

Input:
(i) **Load Transmitted Image E'.**

Extraction Process:
(i) **Apply DWT on Host image E' to get LLx, HLx, LHx, HHx.**
(ii) **Apply second level DWT on LLx sub-band to get LLx2, HLx2, LHx2, HHx2.**
(iii) **Apply SVD on LLx2:** $LLx2 = Ux * Sx * Vx'$.
(iv) **Reconstruct Sw' matrix using:** $Sw' = \frac{(Sx-(1-\alpha^n)*S)}{\alpha^n}$.
(v) **Reconstruct LLw2':** $LLw2' = Uw * Sw' * Vw'$.
(vi) **Apply two times inverse DWT to extract Watermark Image W'.**

Output: Extracted Watermark Image W'

4. Experimental results
In this section proposed scheme is tested and compared with the results obtained using the techniques mentioned in [18][19][20]. The "Peppers" image is used as the host image with default size [256, 256] and "Cameraman" image is used as the watermark image with same size of [256, 256]. The original images are shown in Fig 3 and Fig 4.


Figure 3. Host image: Peppers


Figure 4. Watermark image: Cameraman

4.1. Imperceptibility performance
In evaluation of imperceptibility performance of techniques, the host image is embedded with watermark image and the result image is compared with the host image without any attacks. The embedded image and extracted watermark using the proposed technique are shown in Fig 5 and Fig 6.


Figure 5. Embedded image under no attack


Figure 6. Extracted watermark image

The imperceptibility performance is analysed using quality index metrics mentioned in Table 1.

The results of imperceptibility performance are given in Table 2 and relatively the proposed technique outperforms the existing techniques.

Table 1. Quality metrics for performance evaluation

Quality Metric	Description	Formula	Best Value	Reference
ERGAS	It computes the quality of embedded image in terms of normalized average error of each band of image. Increase in the value of ERGAS indicates disturbance in the embedded image, lower value of ERGAS indicates that the embedded image is similar to the base image.	$100\frac{\mathrm{d}h}{\mathrm{d}l}\left[\frac{1}{n}\sum_{i=1}^{n}\left(\frac{RMSE^2}{mean^2}\right)\right]^{\frac{1}{2}}$	Lower value	(Du et al., 2007) [21]
MSE	It computes the spectral difference between image pixel intensities, the lower value indicates better embedding.	$\frac{1}{N}\sum_{i=1}^{N}(y_i - y_i^{\Lambda})^2$	Lower value	(Pinki et al., 2016)[22]
MSSSIM	The Multi Scale Structural Similarity Index for Motion Detection (MS-SSIM) quality metric is an extension of the SSI which computes these measures at various scales and combines them.	$I_M(x,y)^{\alpha_M}\prod_{i=1}^{n}C_j(x,y)^{\beta_j}S_j(X,y)^{\Upsilon_j}$	Higher Value (Close to unity)	(Z. Wang et al., 2006) [23]
PSNR	It is extensively used metric which is computed by the number of gray levels in the image divided by the corresponding pixels in the base and the embedded images. When the value is high, the base and embedded images are similar. A higher value indicates superior embedding.	$20\log_{10}\left(\frac{L^2}{\frac{1}{MN}\sum_{i=1}^{M}\sum_{j=1}^{N}(Ir(i,j)-If(i,j))^2}\right)$	Higher value	(Naidu, 2010)[24]
RASE	The relative average spectral error (RASE) characterizes the average performance of a method by computing difference between intensities of base image and embedded image. The lower the value, the better the method	$\frac{1}{M}\sqrt{\frac{1}{N}\sum_{i=1}^{N}RMSE^2(B_i)}$	Lower value	(Gonzalez et al., 2003)[25]
RMSE	It is often used to visualise the difference between the base and embedded images by computing the variation in pixel intensities. RMSE gives spectral quality of embedded image.	$\sqrt{\frac{1}{MN}\sum_{i=1}^{M}\sum_{j=1}^{N}(Ir(i,j)-If(i,j))^2}$	Lower value	(Zoran, 2009) [26]

SAM	It computes the spectral angle between the pixel, vector of the base image and embedded image. It is performed on a pixel-by-pixel base. A value of SAM equal to zero denotes the absence of spectral distortion	$arccos\left(\frac{\langle V, V^{\Lambda}\rangle}{\|V\|_2 \cdot \|V^{\Lambda}\|_2}\right)$	Lower value	(Alparone et al., 2007)[27]
UQI	It is used to evaluate the amount of variation of relevant data from base image into embedded image. The range of this metric is -1 to 1. The value 1 indicates that the base and embedded images are similar.	$\left(\frac{4\sigma_{I_r I_f}(\mu_{I_r} + \mu_{I_f})}{(\sigma^2 I_r + \sigma^2 I_f)(\mu^2 I_r + \mu^2 I_f)}\right)$	Higher Value (Close to unity)	(Alparone et al., 2008)[28]
VIFP	VIF measures the mutual information between the base image and embedded image, the higher value indicates the similarity between the images	$\frac{\Sigma_{j \epsilon subbands} I(\overrightarrow{C}^{N,j}; \overrightarrow{F}^{N,j} \| s^{N,j})}{\Sigma_{j \epsilon subbands} I(\overrightarrow{C}^{N,j}; \overrightarrow{E}^{N,j} \| s^{N,j})}$	Higher Value (Close to unity)	(Hamid et. al., 2004)[29]
SSIM	SSIM compares the local patterns of pixel intensities between the base and embedded images. The range varies between -1 to 1.The value 1 indicates the base and embedded images are similar.	$\frac{(2\mu_{I_r}\mu_{I_f} + C_1)(\sigma_{I_r\ I_f} + C_2)}{(\mu^2 I_r + \mu^2 I_f + C_1)(\sigma^2 I_r + \sigma^2 I_f + C_2)}$	Higher Value (Close to unity)	(Wang et al., 2004)[30]

Table 2. Imperceptibility performance of the algorithms.

Quality Metric	**E. Ganic et al.** (Ref: 18)	**Wai CK et al.** (Ref: 19)	**Rahman MN et al.** (Ref: 20)	**Rahman MN et al.** (iterative)	**DWT_SVD_LL2**	**Proposed**
ERGAS	1676.35015	1034.48103	2017.96209	705.4015701	1985.690262	**603.665425**
MSE	33.1715240	6.63858032	29.9302063	2.576126099	29.06634521	**2.11517334**
MSSSIM	0.99611094	0.99875304	0.99862806	0.999314262	0.998920678	**0.99957755**
PSNR	32.9231493	39.9100514	33.3697065	44.02113243	33.49689934	**44.8773439**
RASE	241.960303	149.314475	291.267740	101.8159466	286.6097018	**87.1315989**
RMSE	5.75947254	2.57654426	5.47085060	1.605031495	5.391321287	**1.45436355**
SAM	0.03761580	0.01957114	0.01207048	0.012194174	0.011419176	**0.01105131**
UQI	0.99887454	0.99958285	0.99821040	0.999770130	0.998288749	**0.99985400**
VIFP	0.80328039	0.82015331	0.90898915	0.897728713	**0.912682022**	0.91194932
SSIM	0.98166270	0.99193288	0.99462302	0.995696637	0.995626901	**0.99686668**

4.2. Robustness of technique under attacks

For the analysis of robustness performance, the embedded image is affected by various attacks and the attacked image is used in extraction process. The extracted watermarked image is compared with the original watermark using the same metrics mentioned in imperceptibility performance analysis. The attacks are gaussian blurring with kernel size: 5x5, poison noise, speckle noise, image sharpening, wiener filtering with kernel size: 3x3, average filtering with kernel size: 3x3, median filtering with kernel size: 3x3 and image resizing (256 to 128 and 128 to 256). The performance of proposed model under attacks are shown in Table 3.

Table 3. Performance of proposed algorithm against attacks.

Attack	Attacked image	Extracted watermark
Gaussian blur		
Image sharpening (0.8)	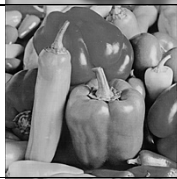	
Average filter (3X3)		
Median filter (3X3)		
Weiner filter (3X3)		
Speckle noise	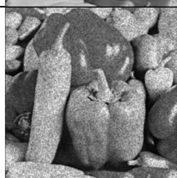	
Resizing (256-128-256)		
Poisson	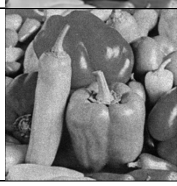	

4.2.1. Gaussian Blur

Gaussian blurring is the outcome of blurring of an image using gaussian function which is implemented by convolving an image with FIR kernel of gaussian values. Mathematical function is given as

$$P(x) = \frac{1}{\sigma\sqrt{2\pi}} e^{-(x-\mu)^2/2\sigma^2} \tag{6}$$

For inspecting the performance of watermarking technique, the embedded image is blurred using gaussian function and the extracted watermark is compared with the original watermark.

4.2.2. Image Sharpening

Image sharpening is used to grab features of an image by maintaining contrast levels of dark and bright. Image is convoluted with the kernel to obtain the smoothed image.

4.2.3. Average Filtering

Average filtering is also referred as smoothening of image, the kernel performs the mean operation for neighbourhood pixels.

4.2.4. Median Filtering

Average filtering is also referred as smoothening of image, the kernel performs the median operation for neighbourhood pixels.

4.2.5. Wiener Filtering

The Wiener filter is the MSE-optimal stationary linear filter for images degraded by additive noise and blurring.

4.2.6. Speckle noise

Speckle noise is defined as multiplicative noise, having a granular pattern it is the inherent property of SAR image.

4.2.7. Resize of image

The embedded image is resized into its lower dimension [128X128] and restored to its original dimension [256X256] to measure its scaling performance.

4.2.8. Poisson Noise

Poisson noise is a signal-dependent noise that can be seen on photon images, and is also called quantum noise.

Table 4. Performance of the algorithms under the attack of Gaussian Blur

ALGORITHM	QUALITY METRIC									
	ERGAS	MSE	MSSSIM	PSNR	RASE	RMSE	SAM	UQI	VIFP	SSIM
E. Ganic et al. - LL (Ref: 18)	49697.39326	5793.661682	-0.0486027103	10.5012723	7173.200845	76.11610659	0.5976222263	0.667047008	0.004555841468	-0.1207801126
E. Ganic et al. - LH (Ref: 18)	45791.1794	17718.4903	0.04457292118	5.64653646	6609.38744	133.11082	1.44715754	0.08135686	0.00089068	0.00881035
E. Ganic et al. - HL (Ref: 18)	45567.4599	17712.2517	0.04247268525	5.64806586	6577.09631	133.087384	1.44111209	0.07655311	0.00084949	0.01654454
E. Ganic et al. - HH (Ref: 18)	45699.6703	17864.5459	0.07046814583	5.6108838	6596.17924	133.658318	1.46628379	0.03912332	0.00033041	0.03460146
Wai CK et al. - LL (Ref: 19)	69571.5545	12467.2232	0.415748381	7.17310627	10041.7889	111.65672	0.6229758	0.57788963	0.15292991	0.2473342
Wai CK et al. - LH (Ref: 19)	67033.18367	10150.69304	0.5789473455	8.065846661	9675.406659	100.7506478	0.3400499968	0.6523511629	**0.1613847108**	0.4156692494
Wai CK et al. - HL (Ref: 19)	78049.6736	10732.779	0.5682136212	7.82368174	11265.5	103.599126	0.35048305	0.65106423	0.1540052	0.41823721
Wai CK et al. - HH (Ref: 19)	43904.2607	15063.8449	0.3985346183	6.35144526	6337.03419	122.734856	0.55589642	0.0300047	0.13784987	0.08288705
Rahman MM et al. (Ref: 20)	30541.6511	2363.27698	0.4272313118	14.3956574	4408.30762	48.6135473	0.36892839	0.80935444	0.03894369	0.0508071
Rahman MM et al. - iterative	21316.5115	1050.85974	0.6844161413	17.9153561	3076.77341	32.4169669	0.24407973	0.87337101	0.09538095	0.30914573
DWT SVD LL2	27814.8153	1637.11177	0.4952803424	15.9900203	4014.72277	40.4612379	0.30648414	0.83647071	0.0495585	0.38939219
Proposed	**18015.3156**	**690.743927**	**0.7472747382**	**19.7376329**	**2600.28683**	**26.2820077**	**0.19628267**	**0.89821301**	0.13642757	**0.62557376**

Table 5. Performance of the algorithms under attack of Sharpen 80

ALGORITHM	QUALITY METRIC									
	ERGAS	MSE	MSSSIM	PSNR	RASE	RMSE	SAM	UQI	VIFP	SSIM
E. Ganic et al. - LL (Ref: 18)	7713.12187	192.283783	0.9290679655	25.291377	1113.29325	13.8666428	0.10235667	0.97295113	0.35702829	0.80145808
E. Ganic et al. - LH (Ref: 18)	25853.884	5480.08928	0.8842457976	10.7429273	3731.68671	74.0276251	0.1163456	0.83413245	0.37524031	0.78229385
E. Ganic et al. - HL (Ref: 18)	25508.0148	5420.47968	0.8851143234	10.7904264	3681.7648	73.623907	0.11571635	0.83595231	0.37936758	0.78579231
E. Ganic et al. - HH (Ref: 18)	29767.7157	6362.61525	0.8778609584	10.094447	4296.59967	79.7660031	0.13189816	0.79682871	0.35523937	0.75696183
Wai CK et al. - LL (Ref: 19)	148635.478	24863.6794	-0.2552630052	4.17514964	21453.6834	157.68221	1.0291628	0.38023674	0.00184271	-0.1187224
Wai CK et al. - LH (Ref: 19)	163255.861	29447.2148	-0.0856249515	3.44036137	23563.9539	171.601908	1.45364246	0.05966168	0.00057897	-0.1247417
Wai CK et al. - HL (Ref: 19)	166985.2348	29955.49182	-0.09271745138	3.366039065	24102.24257	173.076549	1.456165884	0.05730330308	0.0004993717595	-0.1248198069
Wai CK et al. - HH (Ref: 19)	40675.0455	6124.99266	0.735057366	10.2597479	5870.93712	78.2623323	0.17009245	0.74269711	0.23938356	0.53951549
Rahman MM et al. (Ref: 20)	8235.34378	139.3877563	0.9489636273	26.68855733	1188.669487	11.8062592	0.0846099004	0.9353315922	0.4917470125	0.8009392491
Rahman MM et al. - iterative	6641.12499	71.7922363	0.9713735065	29.5700288	958.563826	8.47302994	0.06085041	0.93695972	0.58515592	0.87792956
DWT SVD LL2	3571.27328	29.4524536	0.9848234554	33.4395888	515.468897	5.42701148	0.03910637	0.98502936	0.67167923	0.95813609
Proposed	**1754.30787**	**7.02911377**	**0.9960978853**	**39.6617979**	**253.21253**	**2.65124759**	**0.01926706**	**0.99660973**	**0.83115293**	**0.98863885**

Table 6. Performance of the algorithms under the attack of Average filtering

ALGORITHM	QUALITY METRIC									
	ERGAS	MSE	MSSSIM	PSNR	RASE	RMSE	SAM	UQI	VIFP	SSIM
E. Ganic et al. - LL (Ref: 18)	8574.75539	243.917297	0.9231246367	24.2583776	1237.65933	15.6178519	0.11587146	0.9609788	0.28390028	0.73761809
E. Ganic et al. - LH (Ref: 18)	40600.1106	15179.2255	0.2025413803	6.31830747	5860.1212	123.204	0.52377511	0.1362003	0.00143127	0.14098352
E. Ganic et al. - HL (Ref: 18)	40973.9491	14245.8744	0.2745357919	6.59391251	5914.08014	119.356082	0.37234882	0.10443343	0.0071503	0.13832215
E. Ganic et al. - HH (Ref: 18)	43969.13	16507.8396	0.1695370379	5.95390121	6346.39727	128.482838	0.66074872	0.0513804	0.00077209	0.08012349
Wai CK et al. - LL (Ref: 19)	116675.657	14751.6807	0.3210508784	6.44238857	16840.6805	121.456497	0.60261642	0.62313945	0.07882644	0.15355372
Wai CK et al. - LH (Ref: 19)	77199.2921	12150.5726	0.4251349067	7.28483616	11142.758	110.229636	0.59443478	0.61810917	0.121496	0.2078255
Wai CK et al. - HL (Ref: 19)	63029.85787	14180.04016	0.4111396731	6.614029	9097.576352	119.0799738	0.862043295	0.4495026411	0.1225480271	0.1818951263
Wai CK et al. - HH (Ref: 19)	33155.88879	6784.125366	0.54004198	9.815864961	4785.640329	82.36580216	0.6611952812	0.5400423577	0.1879843307	0.2767740838
Rahman MM et al. (Ref: 20)	7842.885687	98.59918213	0.9596956497	28.19207048	1132.023041	9.929712087	0.0703867141	0.9640206345	0.4500757745	0.8398124724
Rahman MM et al. - iterative	6256.65654	53.1626129	0.9765432617	30.8747404	903.070585	7.29126964	0.05160982	0.97000659	0.58274284	0.92504317
DWT SVD LL2	4065.19869	44.3952332	0.9799783064	31.6574402	586.76089	6.6629748	0.04478901	0.98932909	0.5661497	0.94929498
Proposed	**1712.99868**	**8.40390015**	**0.9964133436**	**38.8859948**	**247.250062**	**2.89894811**	**0.01779372**	**0.99805141**	**0.80751346**	**0.99003718**

Table 7. Performance of the algorithm under the attack of Median filtering

ALGORITHM	QUALITY METRIC									
	ERGAS	MSE	MSSSIM	PSNR	RASE	RMSE	SAM	UQI	VIFP	SSIM
E. Ganic et al. – LL (Ref: 18)	7071.19346	187.185135	0.956988821	25.40809	1020.63886	13.6815619	0.10147099	0.96737433	0.35998295	0.84464613
E. Ganic et al. – LH (Ref: 18)	39614.0555	11654.2617	0.5608274225	7.46595596	5717.7964	107.954906	0.31884477	0.12045585	0.24276181	0.21908065
E. Ganic et al. – HL (Ref: 18)	38472.714	10853.4569	0.5661102203	7.77512276	5553.05794	104.179926	0.21513891	0.1501964	0.26674911	0.24801065
E. Ganic et al. – HH (Ref: 18)	34860.378	9958.09413	0.5530186077	8.14904134	5031.66216	99.7902507	0.10548609	0.2549245	0.25170112	0.34520532
Wai CK et al. – LL (Ref: 19)	129429.256	17947.455	0.1421696681	5.59077487	18681.504	133.968112	0.80145072	0.54663883	0.05074019	0.11159654
Wai CK et al. – LH (Ref: 19)	115216.615	13806.5716	0.3937801353	6.72994512	16630.0859	117.501368	0.48721194	0.63959798	0.10498127	0.23825
Wai CK et al. - HL (Ref: 19)	103905.8422	12717.02109	0.4313881454	7.086949694	14997.51649	112.7697703	0.4506109381	0.6458325214	0.1232031759	0.27224343
Wai CK et al. - HH (Ref: 19)	35414.82683	5491.330292	0.5220505282	10.73402794	5111.689951	74.10351066	0.4852320358	0.6939041672	0.2004685955	0.2719824312
Rahman MM et al. (Ref: 20)	5462.14953	39.6430511	0.9799591178	32.1491329	788.393376	6.2962728	0.04640243	0.97564999	0.60274715	0.9362476
Rahman MM et al. - iterative	4927.40984	30.0313263	0.9841121442	33.3550585	711.210349	5.48008452	0.0404088	0.9771508	0.68454281	0.95709235
DWT SVD LL2	1464.98209	4.89814758	0.9968466241	41.2304849	211.451951	2.2131759	0.01609945	0.99829933	0.82542623	0.9906046
Proposed	**688.555863**	**0.89846802**	**0.9992201559**	**48.5957774**	**99.3844782**	**0.94787553**	**0.00697264**	**0.99953426**	**0.94181189**	**0.99752313**

Table 8. Performance of the algorithms under attack of wiener filtering

ALGORITHM	QUALITY METRIC									
	ERGAS	MSE	MSSSIM	PSNR	RASE	RMSE	SAM	UQI	VIFP	SSIM
E. Ganic et al. - LL (Ref: 18)	7546.98173	214.677567	0.9408379323	24.812937	1089.31298	14.6518793	0.10949229	0.97215681	0.31125757	0.78599792
E. Ganic et al. - LH (Ref: 18)	16690.8194	761.812531	0.8681151971	19.3123225	2409.11227	27.6009516	0.15546246	0.90327547	0.29816757	0.7463261
E. Ganic et al. - HL (Ref: 18)	12131.0342	531.261948	0.8983759539	20.8777165	1750.96396	23.0491203	0.13451255	0.93769139	0.2943549	0.76897941
E. Ganic et al. - HH (Ref: 18)	12067.87	888.83316	0.9310198159	18.6426011	1741.847	29.8133051	0.10436103	0.93658767	0.3655804	0.8272795
Wai CK et al. - LL (Ref: 19)	109112.976	15118.4861	0.3035722674	6.33572055	15749.1015	122.957253	0.70516061	0.59105874	0.07860748	0.14756317
Wai CK et al. - LH (Ref: 19)	93595.9464	12180.4629	0.4192915687	7.27416568	13509.4112	110.365134	0.4811359	0.64757885	0.13506223	0.23392519
Wai CK et al. - HL (Ref: 19)	92562.5452	12052.12718	0.420584982	7.320166549	13360.2526	109.7821806	0.4840268555	0.6477871266	0.1341404777	0.2274485044
Wai CK et al. - HH (Ref: 19)	29067.97794	4197.626495	0.5661670831	11.90076568	4195.601223	64.78909241	0.5030730239	0.6836084041	0.1949100008	0.3039897416
Rahman MM et al. (Ref: 20)	5960.664303	47.41853333	0.9772413881	31.37132244	860.347785	6.886111626	0.05058406845	0.9725241756	0.5783306544	0.9287185142
Rahman MM et al. - iterative	5284.8312	34.2911835	0.982439639	32.7789789	762.799679	5.85586744	0.0431013	0.97481191	0.6651289	0.952541
DWT SVD LL2	1975.94717	8.87069702	0.9953681823	38.6512261	285.203408	2.97837154	0.02142558	0.99657157	0.77992981	0.98722784
Proposed	**842.193823**	**1.5789032**	**0.9990199754**	**46.1472486**	**121.560208**	**1.25654415**	**0.00895**	**0.99936103**	**0.92215018**	**0.99711897**

Table 9. Performance of the algorithms under attack of speckle noise

ALGORITHM	QUALITY METRIC									
	ERGAS	MSE	MSSSIM	PSNR	RASE	RMSE	SAM	UQI	VIFP	SSIM
E. Ganic et al. - LL (Ref: 18)	22375.4924	1431.66393	0.6986437429	16.5723928	3229.62414	37.8373351	0.21790562	0.85707109	0.15829907	0.47818022
E. Ganic et al. - LH (Ref: 18)	29916.06	6407.13689	0.6763307251	10.0641636	4318.01133	80.0445931	0.44125576	0.45909186	0.18539812	0.3650649
E. Ganic et al. - HL (Ref: 18)	31276.0548	7326.16631	0.6441527531	9.48203588	4514.30966	85.5930272	0.48649522	0.41396152	0.17539751	0.34916671
E. Ganic et al. - HH (Ref: 18)	25578.5168	4095.43309	0.6943529246	12.0078053	3691.94089	63.9955709	0.37735699	0.6473315	0.19839249	0.42747906
Wai CK et al. - LL (Ref: 19)	133855.845	21442.8305	-0.0349859643	4.81798249	19320.427	146.433707	0.90895702	0.47977274	0.00235553	-0.0742253
Wai CK et al. - LH (Ref: 19)	156182.875	26421.8465	-0.3249164667	3.91117196	22543.0563	162.547982	1.08105161	0.34126317	0.00158441	-0.1306052
Wai CK et al. - HL (Ref: 19)	161509.954	27372.8376	-0.341368039	3.7576054	23311.9539	165.447386	1.1198701	0.31078596	0.00150651	-0.1321561
Wai CK et al. - HH (Ref: 19)	69976.1362	10673.3283	0.4508396478	7.84780493	10100.1853	103.311801	0.49628987	0.64849443	0.15288497	0.2392179
Rahman MM et al. (Ref: 20)	26681.2358	2107.13249	0.6686621004	14.8938852	3851.10466	45.9035129	0.28822717	0.81628253	0.14902803	0.40885425
Rahman MM et al. - iterative	16193.6222	656.097504	0.8293779116	19.9611198	2337.34803	25.6144003	0.18656338	0.92752025	0.3052101	0.50919595
DWT SVD LL2	20679.6622	1557.49388	0.8050843728	16.2065401	2984.85214	39.465097	0.17178818	0.8514886	0.31681306	0.78790248
Proposed	**2805.95385**	**15.4419556**	**0.9840294175**	**36.2437806**	**405.004553**	**3.92962537**	**0.02931058**	**0.99438379**	**0.69836666**	**0.94356194**

Table 10. Performance of the algorithms under the attack of resizing

ALGORITHM	QUALITY METRIC									
	ERGAS	MSE	MSSSIM	PSNR	RASE	RMSE	SAM	UQI	VIFP	SSIM
E. Ganic et al. - LL (Ref: 18)	7572.24256	195.922333	0.9501021978	25.2099642	1092.95907	13.9972259	0.1030737	0.96482293	0.34639488	0.80969818
E. Ganic et al. - LH (Ref: 18)	46787.1596	17743.6123	0.1499974398	5.64038322	6753.1448	133.205151	1.25901941	0.00328755	0.0009449	0.01524343
E. Ganic et al. - HL (Ref: 18)	46790.6509	17800.291	0.1400738372	5.62653259	6753.64872	133.417731	1.31035655	0.00381739	0.00064996	0.01544224
E. Ganic et al. - HH (Ref: 18)	46239.4267	17889.5037	0.1159251344	5.60482068	6674.08637	133.751649	1.45458606	0.01897751	0.00023348	0.02783459
Wai CK et al. - LL (Ref: 19)	123936.701	17656.5011	0.17872048	5.66175715	17888.722	132.877767	0.82344421	0.54192513	0.04057219	0.09974391
Wai CK et al. - LH (Ref: 19)	89865.6035	11524.9297	0.5698752562	7.51442076	12970.9826	107.354225	0.35630756	0.64061009	0.12779041	0.3918874
Wai CK et al. - HL (Ref: 19)	97259.2995	11955.0244	0.5921852787	7.35529895	14038.1707	109.339034	0.35491897	0.64006055	0.13249348	0.42692672
Wai CK et al. - HH (Ref: 19)	31581.11936	7065.780258	0.596649257	9.639202339	4558.341941	84.05819566	0.6684168288	0.4830349795	0.1970039131	0.3111252835
Rahman MM et al. (Ref: 20)	8775.52836	125.586823	0.9431293806	27.1413629	1266.63842	11.2065527	0.08357372	0.95990018	0.39544812	0.7652682
Rahman MM et al. - iterative	6874.62813	65.8152008	0.9674677868	29.9475415	992.267101	8.11265683	0.0603385	0.96801671	0.50499085	0.8817965
DWT SVD LL2	1853.47225	7.862854	0.9954722777	39.1750015	267.525675	2.8040781	0.02062072	0.99712057	0.78212641	0.98687052
Proposed	**468.980156**	**0.46264648**	**0.9996027321**	**51.4783109**	**67.6914548**	**0.68018121**	**0.00505582**	**0.99980765**	**0.96528382**	**0.99868264**

Table 11. Performance of the algorithms under the attack of poisson noise

ALGORITHM	QUALITY METRIC									
	ERGAS	MSE	MSSSIM	PSNR	RASE	RMSE	SAM	UQI	VIFP	SSIM
E. Ganic et al. - LL (Ref: 18)	11259.8732	396.487152	0.912586737	22.1485124	1625.22271	19.9119851	0.11908418	0.94843644	0.32076248	0.77656218
E. Ganic et al. - LH (Ref: 18)	30021.4268	5867.81317	0.8033962675	10.4460408	4333.21971	76.6016525	0.23574569	0.43743407	0.2832849	0.47299464
E. Ganic et al. - HL (Ref: 18)	31576.4697	6883.23987	0.7683196123	9.75287457	4557.67082	82.9652932	0.24990302	0.37850044	0.26696039	0.43771502
E. Ganic et al. - HH (Ref: 18)	23586.8061	3501.72267	0.8547433006	12.6879861	3404.46222	59.1753553	0.18866975	0.64498075	0.2941959	0.60078162
Wai CK et al. - LL (Ref: 19)	133720.24	22159.2754	-0.08793242435	4.67524805	19300.8541	148.859919	0.9805949	0.43311777	0.00159696	-0.0768571
Wai CK et al. - LH (Ref: 19)	150002.104	25330.0681	-0.2998063625	4.09444003	21650.9388	159.154227	1.05860674	0.36482589	0.00149285	-0.1215388
Wai CK et al. - HL (Ref: 19)	149746.165	25445.4804	-0.3002522788	4.07469707	21613.9972	159.516395	1.07216963	0.35383077	0.00162214	-0.1229487
Wai CK et al. - HH (Ref: 19)	61568.8778	9872.95032	0.4480760675	8.18633409	8886.70205	99.362721	0.5246084	0.65019792	0.15599722	0.23040537
Rahman MM et al. (Ref: 20)	13823.3153	596.663193	0.9068669503	20.3735111	1995.2237	24.4266902	0.10406202	0.92401346	0.42327471	0.81211872
Rahman MM et al. - iterative	5098.26124	55.4287872	0.9739222651	30.6934498	735.870625	7.44505119	0.05488526	0.98772876	0.57860299	0.85247987
DWT SVD LL2	12294.055	490.422089	0.9317857595	21.2251034	1774.49399	22.1454756	0.09588863	0.93493749	0.49416966	0.91430694
Proposed	**781.902471**	**0.97880554**	**0.9984995235**	**48.2238394**	**112.857901**	**0.98934602**	**0.00733461**	**0.99949312**	**0.94240769**	**0.99439084**

5. Conclusions
In this paper, a new robust image watermarking system DWT-SVD domain based on iterative blending is provided to solve the copyright protection problem of a picture. A series of simulation results indicate that the proposed watermarking scheme has good imperceptibility performance without sacrificing the image's quality. Furthermore, the adoption of iterative blending technique highly improved the hiding capacity of the proposed scheme.

6. References

[1] Liu, R.Z.; Tan, T.N.: *An SVD-based watermarking scheme for protecting rightful ownership*. (IEEE transactions, Multimedia) **4**, 121–128 (2002)

[2] Lai, C.C.; Tsai, C.C.: *Digital image watermarking using discrete wavelet transform and singular value decomposition*.(IEEE transactions, Instrumentation and Measurement). **59**, 3060-–3063 (2010).

[3] Gupta, A.K.; Raval, M.S.:*A robust and secure watermarking scheme based on singular values replacement*. (Sadhana) , **37**, 425–440 (2012)

[4] Narula, N.; Sethi, D.; Bhattacharya, P.P.: *Comparative analysis of DWT and DWT-SVD watermarking techniques in RGB images*. (International Journal of Signal Processing, Image Processing and Pattern Recognition). , **8**, 339–348 (2015).

[5] Preda, R.O. *Self-recovery of unauthentic images using a new digital watermarking approach in the wavelet domain*. (In Proceedings of the 2014 10th International Conference on Communications (COMM), Bucharest, Romania); pp. 1–4 (2014)

[6] Hu, J.; Shao, Y.; Ma, W.; Zhang, T.*A robust watermarking scheme based on the human visual system in the wavelet domain*. (In Proceedings of the 2015 8th International Congress on Image and Signal Processing (CISP), Shenyang, China; pp. 799–803) (2015)

[7] Ahmad, A.; Sinha, G.; Kashyap, N. *3-level DWT Image watermarking against frequency and geometrical attacks*. (International Journal of Computer Network and Information Security(IJCNIS)). **6**, 58 (2014)

[8] Hsieh, M., Tseng, D., and Huang, Y. *Hiding digital watermarks using multiresolution wavelet transform*. (IEEE Transactions on Industrial Electronics), **48**(5), 875–882 (2001).

[9] P. Rasti, G. Anbarjafari, and H. Demirel,*Colour image watermarking based on wavelet and QR decomposition*, (in Proceedings. 25th Signal Processing and Communications Applications Conference (SIU)), pp. 1–4 (2017).

[10] Roy, A. K. Maiti, and K. Ghosh,*An HVS inspired robust nonblind watermarking scheme in YCbCr color space*, (International Journal of Image and Graphics), **vol. 18**, no. 3, Art. no. 1850015 (2018).

[11] Y. Lakrissi, A. Saaidi, and A. Essahlaoui,*Novel dynamic color image watermarking based on DWT-SVD and the human visual system*, Multimedia Tools and Applications., **vol. 77**, no. 11, pp. 13531–13555. (2018)

[12] M. Ali and C. W. Ahn,*An optimized watermarking technique based on self-adaptive DE in DWT-SVD transform domain, Signal Process*., **vol. 94**, pp. 545–556 (2014)

[13] W. H. Alshoura, Z. Zainol, J. S. Teh, M. Alawida and A. Alabdulatif, *"Hybrid SVD-Based Image Watermarking Schemes: A Review,"* in IEEE Access, **vol. 9**, pp. 32931–32968 (2021)

[14] Kenneth R. Castleman,*Digital Image Processing*, Tsinghua University Press, pp.331–339, (2003)
[15] B. Zhou and J. Chen.:*A Geometric Distortion Resilient Image Watermarking Algorithm Based on SVD*, Chinese Journal of Image and Graphics, **Vol. 9**, pp. 506–512 (2004)
[16] Zhang Gui-cang, Wang Rang-ding and Zhang Yu-jin.:*Digital Image Information Hiding Technology Based onIterative Blending*, Chinese Journal of Computers, **Vol.25** No.5,pp.569–574 (2003)
[17] R. Gonzalez and R. Woods,*Digital Image Processing*, Prentice Hall, Englewood Cliffs, NJ, (2002).
[18] E. Ganic and A. M. Eskicioglu, *Robust DWT-SVD Domain Image Watermarking: Embedding Data in All Frequencies*, Proceedings of the ACM Multimedia and Security Workshop pp. 166-174, Magdeburg, Germany (2004)
[19] Wai CK, Ahmad NA.: *Robust DWT-SVD image watermarking with hybrid technique for embedding data in all frequencies*. AIP Conference Proceedings (2014)
[20] Rahman MM, Ahammed MS, Ahmed MR, Izhar MN.: *A semi blind watermarking technique for copyright protection of image based on DCT and SVD domain*. The Global Journal of Researches in Engineering **16**(7): 9–15. (2017)
[21] Du, Q., Younan, N.H., King, R., Shah, V.P.:*On the performance evaluation of pan-sharpening techniques*. IEEE Geosci. Remote Sens. Lett. **4**, 518–522 (2007)
[22] Pinki, D.R.Mehra.,*Estimation of the image quality under different distortions*, Int. J. Eng. Sci., **8**, 17291–-17296 (2016).
[23] Z. Wang, E. P. Simoncelli and A. C. Bovik,*"Multiscale structural similarity for image quality assessment,"* The Thrity-Seventh Asilomar Conference on Signals, Systems and Computers, pp. 1398–1402 **Vol.2** (2003).
[24] Naidu, V.P.S.,*Discrete Cosine Transform-based Image Fusion*. Def. Sci. J. **60**, 48–-54 (2010).
[25] M. Gonzalez-Audicana, J. L. Saleta, R. G. Catalan and R. Garcia, *"Fusion of multispectral and panchromatic images using improved IHS and PCA mergers based on wavelet decomposition,"* in IEEE Transactions on Geoscience and Remote Sensing, **vol. 42**, no. 6, pp. 1291–1299,(2004).
[26] Zoran, L.F., . *Quality Evaluation of Multiresolution Remote Sensing Image Fusion*. U.P.B. Sci. Bull., Ser. C **71**, 38–-52 (2009).
[27] Alparone, L., Wald, L., Chanussot, J., Member, S., Thomas, C., Gamba, P., Bruce, L.M., .*Comparison of Pansharpening Algorithms : Outcome of the 2006 GRS-S Data-Fusion Contest*. IEEE Trans. Geosci. Remote SENSINGI **45**, 3012–-3021 (2007).
[28] Alparone, L., Aiazzi, B., Baronti, S., Garzelli, A., Nencini, F., Selva, M.: *Multispectral and Panchromatic Data Fusion Assessment Without Reference*. Photogramm. Eng. Remote Sens. **74**, 193–-200 (2008)
[29] H. R. Sheikh and A. C. Bovik,*"Image information and visual quality,"* in IEEE Transactions on Image Processing, **vol. 15**, no. 2, pp. 430-444 (2006)
[30] Wang, Z., Bovik, A.C., Sheikh, H.R., Member, S., Simoncelli, E.P., Member, S.*Image Quality Assessment : From Error Visibility to Structural Similarity*. IEEE Trans. IMAGE Process. **13**, 1–14 (2004).